



Published in final edited form as:

J Immunol. 2014 June 15; 192(12): 5789–5801. doi:10.4049/jimmunol.1303259.

Targeting antigens through blood dendritic cell antigen 2 (BDCA2) on plasmacytoid dendritic cells promotes immunologic tolerance¹

Craig P. Chappell^{#*}, Natalia V. Giltiay^{#*}, Kevin E. Draves^{*}, ChangHung Chen[‡], Martha S. Hayden-Ledbetter^{*}, Mark J. Shlomchik[§], Daniel H. Kaplan[¶], and Edward A. Clark^{2,*;||}

^{*}Department of Immunology, School of Medicine, University of Washington, Seattle, WA, USA

[‡]EIAb Bio, Gaithersburg MD

[§]Department of Immunology, School of Medicine, University of Pittsburgh, Pittsburgh, PA, USA

[¶]Department of Dermatology, University of Minnesota Medical School, Minneapolis, MN, USA

^{||}Department of Microbiology, School of Medicine, University of Washington, Seattle, WA, USA

[#] These authors contributed equally to this work.

Abstract

The C-type lectin receptor blood dendritic cell antigen 2 (BDCA2) is expressed exclusively on human plasmacytoid dendritic cells (pDCs) and plays a role in Ag capture, internalization and presentation to T cells. We used transgenic mice that express human BDCA2 and anti-BDCA2 mAbs to deliver Ags directly to BDCA2 on pDCs *in vivo*. Targeting Ag to pDCs in this manner resulted in significant suppression of Ag-specific CD4⁺ T cell and Ab responses upon secondary exposure to Ag in the presence of adjuvant. Suppression of Ab responses required both a decrease in effector CD4⁺ T cells and preservation of Foxp3⁺ regulatory T cells (T_{regs}). Reduction in T_{reg} cell numbers following Ag delivery to BDCA2 restored both CD4⁺ T cell activation and Ab responses, demonstrating that T_{regs} were required for the observed tolerance. Our results demonstrate that Ag delivery to pDCs through BDCA2 is an effective method to induce immunological tolerance, which may be useful for treating autoimmune diseases or to inhibit unwanted Ab responses.

INTRODUCTION

A simple approach- Ag targeting- has made it possible to deliver an Ag to a particular dendritic cell (DC)³ subset and thereby program a characteristic immune response: Ag is coupled to a mAb specific for a receptor expressed only or mainly on a DC subpopulation, and then the Ag-mAb complex is injected alone or with an adjuvant (1, 2). Members of the

¹This work was funded by NIH grants AI52203 and AI44257 (E.A.C.) and the Washington State Life Sciences Discovery Fund.

²Address correspondence to: Edward A. Clark, Ph.D., Dept. Immunology, Box 358059, 750 Republican Street, Room E343, University of Washington, Seattle, WA 98109; eaclark@uw.edu; TELEPHONE: 206-543-8706; FAX: 206-616-4274 .

³Abbreviations used in this paper: DC, dendritic cell; CLR, C-type lectin receptor; pDC, plasmacytoid DC; T_{reg}, T regulatory T cell; BDCA2, blood dendritic cell antigen 2; Tg, transgenic; B6, C57BL/6; CGG, chicken gamma globulin; pMHCII, peptide:MHCII.

C-type lectin receptor (CLR) family have been chosen as targets because many CLRs are differentially expressed on DC populations and indeed, have been used for defining DC subsets (3-5). Furthermore, most CLRs internalize after crosslinking and thus, after being bound by Ag-mAbs, can deliver Ags to early endosomes and proteosomes (6-10). Crosslinking of CLRs can also induce characteristic signal transduction pathways and programming of DC subsets (11, 12).

Murine plasmacytoid DCs (pDCs) are a distinct subset of DCs that are phenotypically defined as CD11c^{int}, B220⁺, BST-2⁺ and Siglec-H⁺ (13-16). pDCs were first identified as natural IFN-producing cells due to their ability to secrete high quantities of type I IFNs following either TLR7 or TLR9 engagement by ssRNA and ssDNA viruses, respectively (17-20). Production of type I IFN during infection is critical for establishing an anti-viral state in the host, thereby making pDCs a key component of innate immunity. The contribution of pDCs toward adaptive immunity is more controversial (21). Early reports found that pDCs were poor stimulators of T cells (22), but more recent studies showed that pDCs can indeed present Ags to both CD8⁺ and CD4⁺ T cells (23-25). Furthermore, pDCs can expand and differentiate CD4⁺ T cells into either T_H1, T_H2 or T_H17 cell subsets (26-31). pDCs also can promote the differentiation of Foxp3⁺ regulatory T (T_{reg}) cells in a number of settings (31, 32). The ability of pDCs to act in both tolerogenic and immunogenic ways suggests they may be attractive targets for immunotherapies, including treatment of autoimmune diseases, preventing allograft rejection or promoting anti-tumor responses.

The CLR, blood dendritic cell antigen 2 (BDCA2, CD303 or CLEC4C), is expressed principally on pDCs in humans (33). Cross-linking BDCA2 with mAbs results in receptor internalization, rapid Ca⁺⁺ influx, and signaling via a FcεRIγ-dependent pathway (34-36). To study pDC-mediated immune responses, we utilized mice expressing a human BDCA2 construct (B6.BDCA2) specifically in pDCs together with a novel anti-BDCA2 mAb as a model system to deliver Ag to pDCs *in vivo*. We report that Ag delivered via anti-BDCA2 leads to inhibition of Ag-specific CD4⁺ T cell and Ab responses upon Ag re-challenge. Inhibition of Ag-specific immune responses was a result of both deletion of effector CD4⁺ T cells and concomitant preservation of Foxp3⁺ T_{reg} cells. Both CD4⁺ and Ab responses could be restored by depletion of T_{reg} cells *in vivo*, or through administration of a TLR7 agonist at the time of initial priming, which prevented the deletion of effector CD4⁺ T cells. Our results demonstrate that Ag delivery to BDCA2 expressed on pDCs results in immunological tolerance via a mechanism that requires T_{reg} cells.

MATERIALS AND METHODS

Animals

The human BAC clone RP11-277J24 (Invitrogen) containing the human *Clec4C* promoter and open reading frame was used to generate transgenic FVB mice via standard pronuclear injection. Transgenic (Tg) FVB.BDCA2 mice were backcrossed to H-2^b C57BL/6 (B6) mice for 8 generations to establish the B6.BDCA2 Tg line used in these studies. Transmission of the transgene was determined by PCR using genomic DNA obtained from tail snips (primer 1: 5'-ggg gta cgt tca ttt ttc ttt cc-3'; primer 2: 5'-ttg ggt aat tct gct ccc tga ta-3'). B6 and B6.Ly5.1⁺ OT-II TCR Tg mice with a TCR specific for I-A^b bound to chicken ovalbumin

peptide (amino acids 323-339) were bred and maintained in our laboratory. All animal studies were pre-approved by the University of Washington's Institute for Animal Care and Use Committee.

Immunizations and adoptive transfers

Intravenous injections were administered via the tail or retro-orbital veins in a 200 μ l volume. Formulations of alum plus Ag were prepared according to manufacturer's instructions (Pierce) and administered i.p. in 100-200 μ l volumes. When included, TLR agonists R848 (50 μ g) (Invivogen) or CpG-B ODN1668 (50 μ g) (Invitrogen) were admixed with the Ag and administered as a single i.v. injection. For adoptive transfers, splenocytes from Ly5.1⁺ OT-II TCR transgenic mice containing 1.5×10^6 CD4⁺ V α 2⁺ T cells as determined by flow cytometry were injected i.v. into B6.BDCA2 recipients 1 day prior to immunization.

Generation of anti-BDCA2 mAbs

Hybridomas secreting anti-BDCA2 Abs were generated by the Fred Hutchinson Cancer Research Center's Antibody Development Facility (Seattle, WA) by fusing the Fox-ny fusion partner with splenocytes from RBF/DNJ mice immunized with a BDCA2-mouse Ig fusion protein. Candidate positive wells were identified by screening supernatants on NIH3T3 transfectants stably expressing BDCA2 under the control of the CMV promoter (NIH3T3.BDCA2), generated using a cDNA encoding human BDCA2 kindly provided by Dr. James Arthos (NIAID, Bethesda, MD), followed by testing for binding to human pDCs. We established two clones producing mAbs, UW80.1 and UW80.2 (mouse IgG1), that bound specifically to human pDCs. Anti-BDCA2 mAbs and the mouse IgG1 mAb isotype control G28-1 (specific for human CD37) were prepared from hybridoma supernatants we generated via protein G affinity chromatography columns.

Flow cytometry

$1-2 \times 10^6$ RBC-lysed mouse splenocytes prepared by mechanical disruption of spleens were incubated for 30 min on ice in FACS buffer (1 \times PBS containing 2% FBS) containing varying combinations of biotin- or fluorochrome-conjugated mAbs against Siglec-H, PDCA-1, B220, CD11c, CD8, CD4, CD3, CD19, IgD, NK1.1, V α 2 TCR, Foxp3, CD25, CD44 (all from eBioscience) and CD62L (BD Biosciences). Detection of BDCA2 was performed using AlexaFluor 647-conjugated UW80.1 mAb (eBioscience AlexaFluor647 conjugation kit). Ab-labeled cells were washed 3 \times with FACS buffer followed by detection of biotinylated mAbs using streptavidin-PerCP-Cy5.5 (eBioscience) or streptavidin-FITC (both from BD Biosciences) for 20 min on ice. For Foxp3 detection, the mouse Foxp3 staining kit (eBioscience) was used according to manufacturer's instructions. Apoptotic cells were identified using AnnexinV (eBioscience) according to manufacturer's instructions. Data was acquired using an LSR II or FACScan flow cytometer (BD Biosciences) and analyzed using FlowJo (TreeStar) and Prism (GraphPad) software.

mAb-OVA conjugate preparation

OVA was conjugated in 3-fold molar excess to mAbs via thioether linkages as described (37). Unconjugated OVA was removed from mAb-OVA conjugates using 100 kDa cut-off spin columns (Millipore). Retained mAb-OVA conjugates were resuspended in PBS, treated with polymyxin B (Sigma) overnight at 4C to remove endotoxin, sterile filtered (0.2 μ M) and stored at -20C until use. ELISA assays (described below) were used to confirm Ag-mAb conjugation and determine the final concentration of OVA and mAb. The quantities of OVA per mg of mAb were as follows: OVA-DEC205, 0.86 mg; OVA-G28-1, 0.85 mg; OVA-UW80.1, 0.84 mg; and OVA-Siglec-H, 0.55 mg.

Purification of pDCs and in vitro stimulation

pDCs from single cell suspensions from spleens obtained from B6.BDCA2 mice were enriched using an anti-mPDCA1 microbead isolation kit via treatment with Liberase RI and DNaseI (both from Roche), but otherwise according to the manufacturer's instructions. Enriched pDCs were cultured in 24-well tissue culture plates at 1×10^6 /ml in RPMI-1640 with 50 μ M 2-ME and 10% FCS with either medium only or the indicated mAbs at 2 μ g/ml with or without 20 μ g/ml CpG-A (ODN 2216) for 18 h in a 37°C, 5% CO₂ humidified tissue culture incubator. The following day 800 μ l of supernatants were removed from each well and stored at -80C until use.

ELISA assays

ELISAs were performed as described for measuring OVA- and chicken gamma globulin (CGG)-specific IgM or IgG (38), or OVA-conjugated IgG mAbs (39). For detection of IFN α , high-binding capacity 96-well plates (Immobilon) were coated overnight at 4C with 2.5 μ g/ml rat-anti-mouse IFN α in PBS (PBL InterferonSource). Plates were blocked with PBS containing 0.05% Tween-20 (PBS-T) plus 1% BSA for 2 h at RT, washed with PBS-T, and undiluted or supernatants diluted 1:2 were bound for 2 h at RT. Following 3 washes, rabbit anti-mouse IFN α (PBL InterferonSource) was added for 1 h at RT. Following washes, donkey anti-rabbit-HRP (Jackson Immunoresearch) was added for 1 h at RT followed by 4 washes as above. Concentrations of IFN α were obtained by comparison with known dilutions of universal type I interferon (PBL Biomedical Lab). For detection of IL-12p40, the DuoSet ELISA Kit was used according to manufacturer's instructions (R&D Systems). For confirmation of OVA-mAb conjugation, mAb conjugates were captured with anti-mouse Ig(H+L) (Southern Biotech) and detected with anti-OVA-biotin (Sigma-Aldrich) followed by streptavidin-HRP (R&D Systems). All plates were developed with tetramethylbenzidine substrate (Sigma-Aldrich) and reactions were stopped with addition of equal volume 2N H₂SO₄ (Fisher Scientific). OD₄₅₀ values were obtained on a Model 550 microplate reader (BioRad).

Inhibition of CD25⁺ T_{reg} cells

Mice received two i.p. injections consisting of 500 μ g rat anti-CD25 (PC61.5.3) or IgG1 isotype control Ab (HRPN) (both from BioXCell) at d 3 and d 1 prior to challenge with OVA plus alum. Reduction of Foxp3⁺ CD4⁺ T cells was assessed using flow cytometry by

staining with anti-CD4, anti-Ly5.1 and anti-Foxp3 mAb on d 8 following the final anti-CD25 injection.

RESULTS

Characterization of B6.BDCA2 Tg mice and anti-BDCA2 mAbs

We generated mAbs specific for BDCA2 using spleen cells from mice immunized with a BDCA2-Ig fusion protein (see Materials and Methods). A hybridoma producing a mouse IgG1 mAb, designated UW80.1, was established that bound to NIH-3T3 transfectants stably expressing human BDCA2 (Fig. 1A, **top panel**) and human pDCs (Supplementary Figure 1). UW80.1 blocked the binding by the commercially available anti-BDCA2 mAb AC144 (Miltenyi), suggesting these mAbs recognized the same or overlapping epitopes (Fig. 1A, **bottom panel**).

Tg mice expressing BDCA2 derived from a human BAC clone were generated and backcrossed to B6 mice for at least 8 generations (B6.BDCA2 Tg mice, see Materials and Methods). Flow cytometry analyses of spleens from B6.BDCA2 mice confirmed BDCA2 expression on CD11c^{int} cells that co-expressed Siglec-H, PDCA-1, and B220 (Fig. 1B). BDCA2 was not detected in either B6 (Fig. 1B) or non-Tg littermate controls (data not shown); nor was it detected on T cells, B cells, NK cells, or CD11c^{hi} myeloid DCs from B6.BDCA2 mice (Fig. 1B,C).

Cross-linking BDCA2 on human pDCs inhibits both type I IFN and up-regulation of costimulatory receptors induced by CpG-A or CpG-B stimulation, respectively (40, 41). To determine whether BDCA2 cross-linking in B6.BDCA2 mice behaved similarly, magnetically enriched PDCA-1⁺ pDCs from B6.BDCA2 mice were treated with CpG-A either in the presence or absence of graded doses of anti-BDCA2 (AC144) or isotype control for 24 h. Treatment with anti-BDCA2 significantly inhibited IFN- α production by pDCs in a dose-dependent manner when compared to untreated or isotype control-treated cells (Fig. 1D, **upper panel**). CpG-induced IL-12 production, however, was not suppressed by anti-BDCA2 treatment demonstrating that cytokine responses were not globally affected (Fig. 1D, **lower panel**). Inhibition of IFN- α production by UW80.1 was also observed in additional experiments, although to a lesser extent than with the AC144 mAb (data not shown). Taken together, we conclude that B6.BDCA2 Tg mice display pDC-restricted expression of BDCA2, and that BDCA2 signaling in B6.BDCA2 mice is intact.

Ag delivery to BDCA2 in vivo does not induce Ag-specific Ab responses but does alter the proportions of Ag-specific effector and regulatory T cell subsets

To explore the utility of BDCA2 as a target for Ag delivery, cohorts of B6.BDCA2 mice were injected i.v. with 2 μ g AlexaFluor647-conjugated UW80.1 anti-BDCA2 (α BDCA2-647) or a non-targeting mIgG1 isotype control mAb (isotype-647) and sacrificed 1 h later for analysis by flow cytometry. As shown in Fig. 2A, ~85% of PDCA-1⁺ Siglec-H⁺ splenic pDCs were labeled with α BDCA2-647, whereas less <2% of pDCs bound to isotype-647. A small percentage of CD11c^{hi}PDCA-1^{lo} myeloid DCs (~1%) and CD19⁺IgD⁺ B cells (~1%) bound α BDCA2-647 which was also observed in isotype control-injected

mice, suggesting this minimal binding was Fc γ R-mediated and not due to expression of BDCA2 on these subsets.

To determine whether pDCs can induce Ab responses when Ag is targeted via BDCA2, we coupled OVA to the UW80.1 anti-BDCA2 mAb (OVA-BDCA2), to a mouse IgG1 isotype control (OVA-isotype), or, as a positive control for inducing Ab production after targeting Ag to a DC subset, to anti-DCIR2(OVA-DCIR2) (39); we then immunized groups of B6.BDCA2 mice i.v. with 10 μ g of each construct with or without 50 μ g CpG-B. Serum was collected 10 d later and analyzed for anti-OVA Ab responses by ELISA. Unlike Ag-delivery to DCIR2 on CD8 α ⁻ myeloid DCs (39), neither OVA-BDCA2 nor OVA-isotype induced OVA-specific IgG responses even presence of TLR adjuvants CpG-B (Fig. 2B) or R848 (data not shown).

The lack of Ab responses following OVA-BDCA2 immunization could have been due to a failure to generate CD4⁺ T cell help. Thus, we examined CD4⁺ T cell responses *in vivo* following Ag delivery to BDCA2. OVA-specific Ly5.1⁺ OT-II CD4 T cells were labeled with CFSE and adoptively transferred to cohorts of B6.BDCA2 mice that were injected 24 h later with 1 μ g OVA-BDCA2, OVA-DEC205, OVA-isotype or PBS as a negative control or OVA-DEC205 as a positive control since delivering Ag to DEC205 on CD8 α ⁺ DCs is known to induce CD4⁺ T cell expansion (42, 43) (Fig. 3A). 4 d following immunization, mice were sacrificed, and the frequency of dividing Ly5.1⁺ CD4⁺ OT-II T cells in the spleen was determined by dilution of CFSE using flow cytometry. As expected, administration of OVA-DEC205 induced robust proliferation of OT-II T cells (85.7% \pm 8.2) (44), while injection of PBS or OVA-isotype induced little or no proliferation (PBS: 4.5% \pm 0.8; OVA-isotype: 10.9% \pm 3.7) (Fig. 3B,C). In contrast, a significant proportion of the transferred OT-II T cells divided in response to OVA-BDCA2 compared to OVA-isotype (28.5% \pm 12.2; $p=0.018$) (Fig. 3B,C); however the proliferation index showed that the amount of expansion induced by OVA-BDCA2 was not significantly greater than mice primed with OVA-isotype (Fig. 3D). Despite the induction of modest proliferation, immunization with OVA-BDCA2 resulted in a significant reduction in the frequency (0.29% \pm 0.09 vs. 0.16% \pm 0.05; $p=0.0012$) (Fig. 3E) and total number (Fig. 3F) of transferred OT-II T cells 7 d post-immunization when compared to OVA-isotype control mice. The frequency (Fig. 3E) and number (Fig. 3G) of non-Ag-specific Ly5.1⁻ CD4⁺ T cells were not affected by immunization with OVA-BDCA2 or OVA-isotype. Further analysis using AnnexinV revealed that OVA-BDCA2 administration induced a significant fraction of OT-II T cells to undergo apoptosis on d 4 and 7 post-immunization compared to OVA-isotype-injected controls (Fig. 3H). We conclude that OVA-BDCA2 immunization results in depletion of Ag-specific CD4 T cells.

BDCA2-mediated Ag uptake leads to increased frequencies of Foxp3⁺ T_{reg} cells

pDCs have been implicated in tolerance induction in a number of experimental settings (27, 29, 45, 46). Therefore, following injection of OVA-BDCA2 or OVA-isotype, we quantified the number of OT-II T cells expressing the forkhead box transcription factor Foxp3, a marker for T_{reg} cells. In contrast to the total population of transferred OVA-specific CD4 T cells, the frequency of transferred Ly5.1⁺ T_{reg} cells significantly increased in mice primed

with OVA-BDCA2 (Fig. 4A,B). However, the total number of these cells was not increased compared to OVA-isotype-injected controls (Fig. 4B). We detected no changes in number or frequency of endogenous non-Ag-specific CD4⁺ T cell populations (Fig. 4A,C), suggesting these changes required OVA-specific Ag presentation. In accord with a lack of T_{reg} cell expansion, we detected no significant proliferation of Foxp3⁺ cells by CFSE dilution 4 d following immunization with OVA-BDCA2 (Fig. 4D). The Ly5.1⁺ Foxp3⁺ T_{reg} cells from OVA-BDCA2 treated mice displayed high levels of CD25 and expressed the transcription factor Helios, suggesting these cells were not induced from Foxp3⁻ CD4⁺ T cells (Fig. 4E) (47). Finally, OVA-specific Ly5.1⁺ T_{reg} cells from mice that received OVA-BDCA2 displayed higher amounts of CD44 expression on day 7 p.i. compared to endogenous, non-Ag-specific T_{reg} cells, suggesting Ag delivery to BDCA2 resulted in Ag-specific activation of T_{reg} cells (Fig. 4F). These results demonstrate that OVA-specific Foxp3⁻ CD4⁺ T cells undergo deletion following immunization with OVA-BDCA2, whereas naturally occurring Foxp3⁺ T_{reg} cells are maintained, thereby increasing their relative frequency.

Although we noted increased cell death and a decreased number of transferred Ly5.1⁺ CD4⁺ T cells following OVA-BDCA2 immunization, we could still detect small numbers of these cells as late as d 14 post-immunization (Fig. 3F). Thus, to determine whether Ag-specific CD4⁺ T cells in mice primed with OVA-BDCA2 could respond to a secondary Ag exposure, B6.BDCA2 mice primed with OVA-BDCA2 or OVA-isotype were given 50 µg of OVA precipitated in alum 14 d after the initial priming and analyzed 7 d later by flow cytometry for T cell activation and expansion (scheme shown in Fig. 5A). Transferred OT-II T cells in mice primed with OVA-BDCA2 were again significantly reduced in frequency (Fig. 5B,C) and number (Fig. 5C) following secondary Ag exposure compared to B6.BDCA2 mice primed with OVA-isotype. Furthermore, the frequency of naïve CD44^{lo}CD62L^{hi} OT-II T cells was increased in OVA-BDCA2-primed mice compared to OVA-isotype-injected controls (31.0% ± 7.9 vs. 10.4% ± 4.1; p=0.0004) (Fig. 5B), suggesting that OVA-BDCA2 treatment prevented subsequent Ag-specific T cell activation. In contrast, T_{reg} cells from OVA-BDCA2-primed mice displayed increased frequencies of activated CD44^{hi}CD62L^{lo} cells compared to mice primed with OVA-isotype. Similar to mice injected once with OVA-BDCA2, primed mice that received a secondary Ag challenge displayed a significantly increased frequency of T_{reg} cells due to maintenance of their numbers compared to mice primed with OVA-isotype (Fig. 5D). These results show that the decrease in Ag-specific CD4⁺ T cells induced by OVA-BDCA2, coupled with the maintenance of T_{reg} cells resulted in a significant increase in the ratio of T_{reg}:T_{eff} in mice primed with OVA-BDCA2 (Fig. 5E).

Ag delivery to BDCA2 on pDCs results in Ag-specific tolerance induction

pDCs express several receptors with sufficiently restricted expression to facilitate Ag delivery specifically to them, including Siglec-H (13, 15, 16). To determine whether the increased frequency of T_{regs} seen following Ag delivery to BDCA2 is dependent upon Ag uptake via BDCA2, or rather is a general property of pDCs, we compared Ag targeting to BDCA2 with targeting to Siglec-H. Although DEC205 is expressed on CD8α⁺ myeloid DCs (and not pDCs), we also targeted this receptor because it has been shown under some conditions to induce T_{reg} cells *de novo* (48, 49). Priming mice with OVA-DEC205 or OVA-

BDCA2, as expected, led to significantly increased frequencies of T_{reg} cells (Fig. 5F). In contrast, priming mice with OVA-Siglec-H failed to increase T_{reg} frequencies, which remained similar to OVA-isotype controls as reported previously (46). These results demonstrate that Ag delivery to BDCA2 leads to a different outcome than when Ag is delivered to Siglec-H, and that deletion of Ag-specific CD4⁺ T cells is not a universal outcome following Ag delivery to pDCs in B6.BDCA2 mice.

Although Ag delivery to Siglec-H did not increase the frequency of T_{reg} cells, it nonetheless has been shown to inhibit Ab responses to subsequent challenge with Ag (46). The decrease in total numbers of OT-II CD4⁺ cells together with the maintenance of T_{reg} cells following OVA-BDCA2 treatment suggested that mice primed with OVA-BDCA2 may be unable to mount Ab responses to specific Ag. To test this possibility, we quantified OVA-specific Ab responses in mice primed with OVA-BDCA2 or OVA-isotype following exposure to Ag plus alum. Groups of B6.BDCA2 mice were primed with OVA-BDCA2, OVA-isotype, PBS or OVA precipitated in alum, re-challenged 14 d later with OVA plus alum and monitored weekly for OVA-specific Ab responses (see scheme in Fig. 6A). Mice primed with PBS, OVA-isotype or OVA plus alum mounted significant anti-OVA Ab responses following the Ag boost (Fig. 6B). In contrast, anti-OVA Ab responses in mice primed with OVA-BDCA2 were significantly inhibited compared to mice primed with OVA-isotype ($p < 0.0001$ at d 28 p.i.) or PBS ($p = 0.037$ at d 28 p.i.) (Fig. 6B). The inhibition of Ab responses induced by Ag delivery to BDCA2 was Ag-specific as mice primed with OVA-BDCA2 remained capable of mounting Ab responses to an unrelated Ag, CGG, when administered in alum (Fig. 6C). These results demonstrate that Ag uptake via BDCA2 in the absence of other costimulation induces a form of Ag-specific tolerance capable of inhibiting Ab responses.

T_{reg} cells are required for BDCA2-mediated inhibition of Ab responses

The mechanism underlying inhibition of Ab responses following Ag uptake by BDCA2 could be mediated by T_{reg} cells because, unlike Foxp3⁻ CD4⁺ T cells, the number of T_{reg} cells are maintained following treatment with OVA-BDCA2. Alternatively, the deletion of Ag-specific Foxp3⁻ CD4⁺ T cells we observe may be sufficient to prevent an Ag-specific response from occurring, which would not be expected to require T_{reg} cells. To distinguish between these two possibilities, we administered anti-CD25 mAb (PC61) to inhibit the activity of T_{reg} cells in mice that had been treated with OVA-BDCA2 or OVA-isotype (50). Mice were primed with OVA-BDCA2 or OVA-isotype, administered anti-CD25 mAb or isotype control on d -3 and -1 prior to re-challenge with OVA plus alum, and bled weekly following the re-challenge or, in some cases, analyzed 7 d post-challenge for T cell responses (scheme shown in Fig. 7A).

Flow cytometry analyses of splenocytes 7 d post-boost (8 d post-depletion) showed that injection of anti-CD25 mAb resulted in a ~38% reduction in the frequency of Foxp3⁺ T cells compared to isotype control-injected animals (Fig. 7B,C). Anti-CD25 treatment did not significantly affect the total number of transferred Ly5.1⁺ (Fig. 7D) or endogenous Ly5.1⁻ CD4⁺ T cells (Fig. 7B). In OVA-BDCA2-treated mice that did not receive anti-CD25 mAb, the frequency of activated CD44^{hi} CD4⁺ T cells was significantly decreased compared to OVA-isotype controls (Fig. 7E,F). In contrast, treatment with anti-CD25 mAb significantly

increased the fraction of activated OT-II T cells in OVA-BDCA2-primed mice, but not in OVA-isotype-immunized controls. (Fig. 7E,F). Importantly, inhibition of T_{reg} cell activity with anti-CD25 restored anti-OVA Ab responses in OVA-BDCA2-primed mice to levels similar to that of isotype control-treated mice primed with OVA-isotype (“untreated” control group) (Fig. 7G). These results demonstrate that Foxp3⁺ T_{reg} cells are required for the inhibition of Ag-specific CD4⁺ T cell activation and Ab responses induced by delivering Ag to BDCA2 on pDCs.

Ag uptake under inflammatory conditions prevents BDCA2-mediated tolerance induction

pDCs can be activated by a number of pathogen sensing receptors, including TLR7 and TLR9. Administration of the TLR7 agonist R848 to B6.BDCA2 mice induced upregulation of multiple costimulatory molecules on the pDC surface including CD80, CD86, MHCII, and CD40. Unlike TLR7 ligation, cross-linking BDCA2 by UW80.1 mAb did not induce pDC activation, and did not affect TLR7-mediated upregulation of costimulatory molecules (Supplementary Figure 2). To determine whether TLR7 stimulation of pDCs at the time of immunization could abrogate BDCA2-mediated tolerance, B6.BDCA2 mice were immunized as in Fig. 3A with or without 50 µg R848 and analyzed for subsequent T and B cell responses. In contrast to mice primed with OVA-BDCA2 alone, the frequency and number of transferred OT-II cells 7 d p.i. was not reduced in mice given R848 (Fig. 8A), but were instead maintained and similar to those in mice primed with OVA-isotype (either with or without R848). Mice given OVA-BDCA2 plus R848 had a reduced frequency, but not number, of T_{reg} cells compared to mice given OVA-BDCA2 alone (Fig. 8B). This resulted in a T_{reg}:T_{eff} ratio that was similar to OVA-isotype control mice and significantly greater than mice that received OVA-BDCA2 alone (Fig. 8C). Importantly, mice that received R848 together with OVA-BDCA2 mounted significant Ab responses 14 days following re-challenge with OVA plus alum, in contrast to mice primed with OVA-BDCA2 alone (Fig. 8D). We conclude from these results that administration of a TLR7 agonist at the time of initial Ag exposure prevents the deletion of Foxp3⁻ CD4 T cells and inhibition of Ab responses induced by BDCA2-mediated Ag uptake.

DISCUSSION

We found that Ag attached to an Ab against the human CLR, BDCA2, can induce Ag-specific tolerance when injected *in vivo* via a mechanism requiring T_{reg} cells. The data shown herein using a mouse model expressing human BDCA2 strongly suggest that Ag targeting to BDCA2 in humans may be useful for inducing tolerance to prevent adverse Ab responses. Recently, Macauley *et al.* demonstrated Ag-specific inhibition of Ab responses by induction of B cell tolerance via simultaneous engagement of BCR and the inhibitory BCR co-receptor CD22 (51). The benefit of being able to inhibit Ag-specific Ab production was demonstrated in a model of hemophilia, where anti-Factor VIII antibodies prohibit replacement therapy with exogenous Factor VIII. Our analogous data here show that Ag-specific inhibition of Ab responses can also be achieved by delivering Ag to BDCA2 expressed by pDCs, a cell type known to possess both activating and tolerogenic properties.

The tolerogenic nature of pDCs has been demonstrated in a variety of experimental settings including graft versus host disease, tumors, asthma and rheumatoid arthritis (52-55). The induction of tolerance by pDCs has been linked in many cases with their ability to induce the differentiation or development of T_{reg} cells and/or IL-10-producing CD4 T cells (reviewed in (32)). pDCs use multiple mechanisms to induce T_{reg} cell differentiation and/or suppression of T_{eff} cell responses including pDC-mediated production of indoleamine 2,3-dioxygenase, ICOS-L-mediated induction of IL-10-producing T cells, and secretion of granzyme B (28, 56, 57). Thus far the suppressive functions of pDCs and their ability to induce or support T_{reg} cell differentiation and immunological tolerance have almost exclusively been demonstrated *in vitro* or through pDC depletion studies. In our study, we took a different approach by targeting Ag directly to pDCs *in vivo* and assessed Ab and T cell responses following immunization.

Ag delivery to BDCA2 failed to induce Ag-specific Ab responses even when delivered together with CpG-B. Analysis of Ag-specific CD4 T cell responses revealed that OVA-BDCA2 treatment in the absence of adjuvant induced weak proliferation of Ag-specific CD4 T cells that was accompanied by significant cell death. Cumulatively, this resulted in decreased numbers of OVA-specific CD4⁺ T cells in mice that received OVA-BDCA2 compared to OVA-isotype controls. The decrease in Ag-specific CD4⁺ T cells was not uniform, however, because the number of OVA-specific Foxp3⁺ T_{reg} cells did not decrease together with Foxp3⁻ CD4⁺ T cells, but were instead maintained. This scenario was preserved (and somewhat pronounced) following re-challenge of OVA-BDCA2-primed mice with Ag plus alum. The combined loss of Foxp3⁻ T_{eff} cells and maintenance of T_{reg} cells resulted in an increased ratio of T_{reg}:T_{eff} cells in OVA-BDCA2-primed mice that was sufficient to significantly suppress both CD4⁺ T cell activation (Fig. 5) and Ab responses (Fig. 6) upon secondary Ag challenge with adjuvant. The maintenance of Foxp3⁺ T_{reg} cells following immunization with OVA-BDCA2 was required for tolerance induction because inhibiting their activity via anti-CD25 injection after OVA-BDCA2 priming abrogated the inhibition of Ab responses and CD4⁺ T cell activation upon Ag re-challenge (Fig. 7). Therefore, both the deletion of Foxp3⁻ CD4⁺ T cells following OVA-BDCA2 treatment, together with maintenance of T_{reg} cells, was required for the suppression of immune responses induced by Ag delivery to BDCA2.

We found that targeting Ag to BDCA2 in the presence of R848 (a TLR7 agonist) *in vivo* prevented the deletion of Foxp3⁻ CD4⁺ T cells and altered the T_{reg}:T_{eff} ratio such that mice were no longer tolerized and consequently were able to mount Ab responses to a secondary Ag challenge. This change in response correlated with TLR7-induced upregulation of multiple costimulatory molecules on pDCs (Supplementary Figure 2) and supports the notion that Ag presentation by pDCs in the absence of costimulation leads to effector T cell depletion. Thus, tolerance induction via Ag delivery to BDCA2 was prevented if TLR-driven inflammation was induced at the same time.

Although we have been able to demonstrate the effect of Ag targeting to a human pDC receptor *in vivo*, further studies are required to understand how Ag delivery to BDCA2 induces tolerance compared to Ag delivery to other receptors. Our results thus far suggest BDCA2-mediated tolerance induction may operate via a distinct mechanism compared to

what occurs after Ag targeting to other receptors (1). Ag delivery to DEC205 on CD8 α^+ DCs, when administered in low doses in the absence of adjuvant, induces CD4 $^+$ T cell tolerance mediated by *de novo* induction of T_{reg} cells (48). We did not detect *de novo* induction of T_{reg} cells after targeting Ag to BDCA2, yet the frequencies of Foxp3 $^+$ T_{reg} cells and the ratio of T_{reg}:T_{eff} cells in mice primed with OVA-BDCA2 were similar to those induced by OVA-DEC205 administration (Fig. 5). Loschko *et al.* recently showed that Ag delivery to pDC-restricted Siglec-H can also induce tolerance and mediate suppression of Ab responses to subsequent Ag exposure (46). Tolerance induction following Ag delivery to Siglec-H did not involve *de novo* induction of T_{reg} cells. Instead, Ag delivery to Siglec-H resulted in low levels of persistent surface peptide:MHCII complexes (pMHCII) that drove the proliferation and functional exhaustion of Ag-specific CD4 $^+$ T_{eff} cells.

Jaehn *et al.* previously showed that targeting Ag to BDCA2 on activated human pDCs *in vitro* led to presentation of CMV-derived Ags on MHC class II that resulted in proliferation and differentiation of CMV-specific autologous memory CD4 $^+$ T cells (34, 41). Similar findings in the human system have been reported when targeting tetanus toxoid or keyhole limpet hemocyanin to DCIR, FcR and DEC205 on human pDCs activated *in vitro* (58-60). Ag internalized by these receptors must enter into the late-endosomal/lysosomal Ag pathway for degradation and presentation on MHC class II. It was recently shown that binding of mAbs to the transferrin receptor redirects its native intracellular trafficking (i.e., when bound by its natural ligand, transferrin) from recycling endosomes to late endosomal compartments (61). The extent to which mAb binding affects the internalization pathways of receptors such as BDCA2 and Siglec-H is not known and may be one factor that contributes to the differences in outcomes following targeting Ag to different receptors on pDCs (1).

One question stemming from our findings is why are CD4 T_{eff} cells deleted while Foxp3 $^+$ CD4 $^+$ T_{reg} cells are maintained? One possible clue is that the deletion of CD4 $^+$ T cells seen following Ag delivery to BDCA2 correlated with pDC activation status: ligation of BDCA2 by UW80.1 mAbs *in vivo* did not induce upregulation of costimulatory molecules required for CD4 T cell activation including CD80, CD86, MHC II, or CD40 (Supplementary Figure 2), or alter expression of receptors associated with tolerogenic pDCs such as CCR9, CD9 and Fas. Surface expression of costimulatory molecules, however, was strongly increased when the TLR7 agonist R848 was included at the time of OVA-BDCA2 immunization. These results are consistent with a scenario in which Ag presentation following Ag targeting to BDCA2 without significant costimulation, leads to T_{eff} cell deletion. T_{reg} cells, on the other hand, are hyporesponsive to TCR signals due to constitutive expression of CTLA-4 and recruitment of phosphatases by its intracellular domain (62-65). Such constitutive CTLA-4 expression by T_{reg} cells may have prevented the induction of activation-induced cell death that occurs with CD4 T_{eff} cells. Further studies are required to define both the mechanism of CD4 T_{eff} cell death following BDCA2-mediated Ag presentation and why Foxp3 $^+$ CD4 T cells are refractory to deletion.

In conclusion, our data show that Ag delivery to BDCA2 expressed by pDCs has the ability to promote Ag-specific immune tolerance by altering the balance between T_{eff} and T_{reg} cell populations. Deletion of Ag-specific Foxp3 $^-$ CD4 $^+$ T cells and simultaneous maintenance of naturally occurring T_{reg} cells were both required for BDCA2-mediated tolerance induction,

a mechanism which differs from that described for tolerance induction following Ag delivery to Siglec-H and DEC205 (46, 48). It is noteworthy that recently a similar shift toward an increased ratio of CD4⁺ T_{reg}:T_{eff} cells was found in type 1 diabetes patients treated in a phase 2 clinical trial with a CD2 blocker, alefacept (LFA3-Ig) (66). The authors suggested that ‘By targeting the most pathogenic T cells, while sparing T_{regs}, alefacept might contribute to reestablishing a state of immune tolerance’. It will be of interest to determine if an Ag-specific BDCA2-based therapeutic is beneficial for treating certain autoimmune diseases. BDCA2-mediated tolerance induction could be abrogated by inhibiting the activity of Foxp3⁺ T_{reg} cells, or prevented if deletion of Foxp3⁻ CD4⁺ T cells was mitigated by co-administration of a TLR7 agonist at the time of immunization. Thus, Ag uptake by BDCA2 under inflammatory conditions (TLR stimulation) may lead to immune activation vs. tolerance. These data contribute to the growing body of evidence demonstrating pDCs as a powerful subset of cells that possess strong immune modulating properties, making them attractive targets for future therapies aimed at manipulating immune responses.

Supplementary Material

Refer to Web version on PubMed Central for supplementary material.

Acknowledgments

We would like to thank Dr. Estelle Bettelli for helpful discussions concerning administration of PC61 mAb.

REFERENCES

1. Chappell CP, Giltiay NV, Dresch C, Clark EA. Controlling immune responses by targeting antigens to dendritic cell subsets and B cells. *Int Immunol*. 2014; 26:3–11. [PubMed: 24285828]
2. Caminschi I, Lahoud MH, Shortman K. Enhancing immune responses by targeting antigen to DC. *Eur J Immunol*. 2009; 39:931–938. [PubMed: 19197943]
3. Kreutz M, Tacke PJ, Figdor CG. Targeting dendritic cells--why bother? *Blood*. 2013; 121:2836–2844. [PubMed: 23390195]
4. Geijtenbeek TB, van Vliet SJ, Engering A, Hart BA, van Kooyk Y. Self- and nonself-recognition by C-type lectins on dendritic cells. *Annu Rev Immunol*. 2004; 22:33–54. [PubMed: 15032573]
5. Garcia-Vallejo JJ, van Kooyk Y. The physiological role of DC-SIGN: A tale of mice and men. *Trends Immunol*. 2009; 34:482–486. [PubMed: 23608151]
6. Pyz E, Marshall AS, Gordon S, Brown GD. C-type lectin-like receptors on myeloid cells. *Ann Med*. 2006; 38:242–251. [PubMed: 16754255]
7. Engering A, Geijtenbeek TB, van Vliet SJ, Wijers M, van Liempt E, Demaurex N, Lanzavecchia A, Fransen J, Figdor CG, Piguet V, van Kooyk Y. The dendritic cell-specific adhesion receptor DC-SIGN internalizes antigen for presentation to T cells. *J Immunol*. 2002; 168:2118–2126. [PubMed: 11859097]
8. Gijzen K, Cambi A, Torensma R, Figdor CG. C-type lectins on dendritic cells and their interaction with pathogen-derived and endogenous glycoconjugates. *Curr Protein Pept Sci*. 2006; 7:283–294. [PubMed: 16918443]
9. Burgdorf S, Kautz A, Bohnert V, Knolle PA, Kurts C. Distinct pathways of antigen uptake and intracellular routing in CD4 and CD8 T cell activation. *Science*. 2007; 316:612–616. [PubMed: 17463291]
10. Schreibelt G, Klinkenberg LJ, Cruz LJ, Tacke PJ, Tel J, Kreutz M, Adema GJ, Brown GD, Figdor CG, de Vries IJ. The C-type lectin receptor CLEC9A mediates antigen uptake and

- (cross-)presentation by human blood BDCA3+ myeloid dendritic cells. *Blood*. 2008; 119:2284–2292. [PubMed: 22234694]
11. Sancho D, Reis e Sousa C. Signaling by myeloid C-type lectin receptors in immunity and homeostasis. *Annu Rev Immunol*. 2012; 30:491–529. [PubMed: 22224766]
 12. Kerrigan AM, Brown GD. Syk-coupled C-type lectins in immunity. *Trends Immunol*. 2011; 32:151–156. [PubMed: 21334257]
 13. Zhang J, Raper A, Sugita N, Hingorani R, Salio M, Palmowski MJ, Cerundolo V, Crocker PR. Characterization of Siglec-H as a novel endocytic receptor expressed on murine plasmacytoid dendritic cell precursors. *Blood*. 2006; 107:3600–3608. [PubMed: 16397130]
 14. Nakano H, Yanagita M, Gunn MD. CD11c(+)B220(+)Gr-1(+) cells in mouse lymph nodes and spleen display characteristics of plasmacytoid dendritic cells. *J Exp Med*. 2001; 194:1171–1178. [PubMed: 11602645]
 15. Blasius AL, Giurisato E, Cella M, Schreiber RD, Shaw AS, Colonna M. Bone marrow stromal cell antigen 2 is a specific marker of type I IFN-producing cells in the naive mouse, but a promiscuous cell surface antigen following IFN stimulation. *J Immunol*. 2006; 177:3260–3265. [PubMed: 16920966]
 16. Blasius AL, Cella M, Maldonado J, Takai T, Colonna M. Siglec-H is an IPC-specific receptor that modulates type I IFN secretion through DAP12. *Blood*. 2006; 107:2474–2476. [PubMed: 16293595]
 17. Siegal FP, Kadowaki N, Shodell M, Fitzgerald-Bocarsly PA, Shah K, Ho S, Antonenko S, Liu YJ. The nature of the principal type 1 interferon-producing cells in human blood. *Science*. 1999; 284:1835–1837. [PubMed: 10364556]
 18. Kadowaki N, Antonenko S, Lau JY, Liu YJ. Natural interferon alpha/beta-producing cells link innate and adaptive immunity. *J Exp Med*. 2000; 192:219–226. [PubMed: 10899908]
 19. Cella M, Jarrossay D, Facchetti F, Alebardi O, Nakajima H, Lanzavecchia A, Colonna M. Plasmacytoid monocytes migrate to inflamed lymph nodes and produce large amounts of type I interferon. *Nat Med*. 1999; 5:919–923. [PubMed: 10426316]
 20. Barchet W, Cella M, Odermatt B, Asselin-Paturel C, Colonna M, Kalinke U. Virus-induced interferon alpha production by a dendritic cell subset in the absence of feedback signaling in vivo. *J Exp Med*. 2002; 195:507–516. [PubMed: 11854363]
 21. Villadangos JA, Young L. Antigen-presentation properties of plasmacytoid dendritic cells. *Immunity*. 2008; 29:352–361. [PubMed: 18799143]
 22. Krug A, Veeraswamy R, Pekosz A, Kanagawa O, Unanue ER, Colonna M, Cella M. Interferon-producing cells fail to induce proliferation of naive T cells but can promote expansion and T helper 1 differentiation of antigen-experienced unpolarized T cells. *J Exp Med*. 2003; 197:899–906. [PubMed: 12668648]
 23. Tel J, Lambeck AJ, Cruz LJ, Tacken PJ, de Vries IJ, Figdor CG. Human plasmacytoid dendritic cells phagocytose, process, and present exogenous particulate antigen. *J Immunol*. 2010; 184:4276–4283. [PubMed: 20304825]
 24. Di Pucchio T, Chatterjee B, Smed-Sorensen A, Clayton S, Palazzo A, Montes M, Xue Y, Mellman I, Banchereau J, Connolly JE. Direct proteasome-independent cross-presentation of viral antigen by plasmacytoid dendritic cells on major histocompatibility complex class I. *Nat Immunol*. 2008; 9:551–557. [PubMed: 18376401]
 25. Salio M, Palmowski MJ, Atzberger A, Hermans IF, Cerundolo V. CpG-matured murine plasmacytoid dendritic cells are capable of in vivo priming of functional CD8 T cell responses to endogenous but not exogenous antigens. *J Exp Med*. 2004; 199:567–579. [PubMed: 14970182]
 26. Yu CF, Peng WM, Oldenburg J, Hoch J, Bieber T, Limmer A, Hartmann G, Barchet W, Eisehubinger AM, Novak N. Human plasmacytoid dendritic cells support Th17 cell effector function in response to TLR7 ligation. *J Immunol*. 2010; 184:1159–1167. [PubMed: 20026744]
 27. Loschko J, Krug A. Antigen delivery to plasmacytoid dendritic cells – induction of tolerance and immunity. *Crit Rev Immunol*. 2012; 32:489–501. [PubMed: 23428225]
 28. Ito T, Yang M, Wang YH, Lande R, Gregorio J, Perng OA, Qin XF, Liu YJ, Gilliet M. Plasmacytoid dendritic cells prime IL-10-producing T regulatory cells by inducible costimulator ligand. *J Exp Med*. 2007; 204:105–115. [PubMed: 17200410]

29. Moseman EA, Liang X, Dawson AJ, Panoskaltis-Mortari A, Krieg AM, Liu YJ, Blazar BR, Chen W. Human plasmacytoid dendritic cells activated by CpG oligodeoxynucleotides induce the generation of CD4+CD25+ regulatory T cells. *J Immunol.* 2004; 173:4433–4442. [PubMed: 15383574]
30. Boonstra A, Asselin-Paturel C, Gilliet M, Crain C, Trinchieri G, Liu YJ, O'Garra A. Flexibility of mouse classical and plasmacytoid-derived dendritic cells in directing T helper type 1 and 2 cell development: dependency on antigen dose and differential toll-like receptor ligation. *J Exp Med.* 2003; 197:101–109. [PubMed: 12515817]
31. Kawamura K, Kadowaki N, Kitawaki T, Uchiyama T. Virus-stimulated plasmacytoid dendritic cells induce CD4+ cytotoxic regulatory T cells. *Blood.* 2006; 107:1031–1038. [PubMed: 16219801]
32. Swiecki M, Colonna M. Unraveling the functions of plasmacytoid dendritic cells during viral infections, autoimmunity, and tolerance. *Immunol Rev.* 2010; 234:142–162. [PubMed: 20193017]
33. Dzionek A, Fuchs A, Schmidt P, Cremer S, Zysk M, Miltenyi S, Buck DW, Schmitz J. BDCA-2, BDCA-3, and BDCA-4: three markers for distinct subsets of dendritic cells in human peripheral blood. *J Immunol.* 2000; 165:6037–6046. [PubMed: 11086035]
34. Jaehn PS, Zaenker KS, Schmitz J, Dzionek A. Functional dichotomy of plasmacytoid dendritic cells: antigen-specific activation of T cells versus production of type I interferon. *Eur J Immunol.* 2008; 38:1822–1832. [PubMed: 18581320]
35. Dzionek A, Sohma Y, Nagafune J, Cella M, Colonna M, Facchetti F, Gunther G, Johnston I, Lanzavecchia A, Nagasaka T, Okada T, Vermi W, Winkels G, Yamamoto T, Zysk M, Yamaguchi Y, Schmitz J. BDCA-2, a novel plasmacytoid dendritic cell-specific type II C-type lectin, mediates antigen capture and is a potent inhibitor of interferon alpha/beta induction. *J Exp Med.* 2001; 194:1823–1834. [PubMed: 11748283]
36. Cao W, Zhang L, Rosen DB, Bover L, Watanabe G, Bao M, Lanier LL, Liu YJ. BDCA2/Fc epsilon RI gamma complex signals through a novel BCR-like pathway in human plasmacytoid dendritic cells. *PLoS Biol.* 2007; 5:e248. [PubMed: 17850179]
37. Weir DM, Herzenberg LA, Blackwell C, Herzenberg LA. *Handbook of Experimental Immunology.* 1986; 1:31.36–37.
38. Goins CL, Chappell CP, Shashidharamurthy R, Selvaraj P, Jacob J. Immune complex-mediated enhancement of secondary antibody responses. *J Immunol.* 2010; 184:6293–6298. [PubMed: 20439912]
39. Chappell CP, Draves KE, Giltiay NV, Clark EA. Extrafollicular B cell activation by marginal zone dendritic cells drives T cell-dependent antibody responses. *J Exp Med.* 2012; 209:1825–1840. [PubMed: 22966002]
40. Kerkmann M, Rothenfusser S, Hornung V, Towarowski A, Wagner M, Sarris A, Giese T, Endres S, Hartmann G. Activation with CpG-A and CpG-B oligonucleotides reveals two distinct regulatory pathways of type I IFN synthesis in human plasmacytoid dendritic cells. *J Immunol.* 2003; 170:4465–4474. [PubMed: 12707322]
41. Jahn PS, Zanker KS, Schmitz J, Dzionek A. BDCA-2 signaling inhibits TLR-9-agonist-induced plasmacytoid dendritic cell activation and antigen presentation. *Cell Immunol.* 2010; 265:15–22. [PubMed: 20673884]
42. Carter RW, Thompson C, Reid DM, Wong SY, Tough DF. Preferential induction of CD4+ T cell responses through in vivo targeting of antigen to dendritic cell-associated C-type lectin-1. *J Immunol.* 2006; 177:2276–2284. [PubMed: 16887988]
43. Lahoud MH, Ahmet F, Kitsoulis S, Wan SS, Vremec D, Lee CN, Phipson B, Shi W, Smyth GK, Lew AM, Kato Y, Mueller SN, Davey GM, Heath WR, Shortman K, Caminschi I. Targeting Antigen to Mouse Dendritic Cells via Clec9A Induces Potent CD4 T Cell Responses Biased toward a Follicular Helper Phenotype. *J Immunol.* 2011
44. Hawiger D, Inaba K, Dorsett Y, Guo M, Mahnke K, Rivera M, Ravetch JV, Steinman RM, Nussenzweig MC. Dendritic cells induce peripheral T cell unresponsiveness under steady state conditions in vivo. *J Exp Med.* 2001; 194:769–779. [PubMed: 11560993]
45. Matta BM, Castellana A, Thomson AW. Tolerogenic plasmacytoid DC. *Eur J Immunol.* 2010; 40:2667–2676. [PubMed: 20821731]

46. Loschko J, Heink S, Hackl D, Dudziak D, Reindl W, Korn T, Krug AB. Antigen targeting to plasmacytoid dendritic cells via Siglec-H inhibits Th cell-dependent autoimmunity. *J Immunol.* 2011; 187:6346–6356. [PubMed: 22079988]
47. Thornton AM, Korty PE, Tran DQ, Wohlfert EA, Murray PE, Belkaid Y, Shevach EM. Expression of Helios, an Ikaros transcription factor family member, differentiates thymic-derived from peripherally induced Foxp3+ T regulatory cells. *J Immunol.* 2010; 184:3433–3441. [PubMed: 20181882]
48. Yamazaki S, Dudziak D, Heidkamp GF, Fiorese C, Bonito AJ, Inaba K, Nussenzweig MC, Steinman RM. CD8+ CD205+ splenic dendritic cells are specialized to induce Foxp3+ regulatory T cells. *J Immunol.* 2008; 181:6923–6933. [PubMed: 18981112]
49. Kretschmer R, Heng TS, von Boehmer H. De novo production of antigen-specific suppressor cells in vivo. *Nat Protoc.* 2006; 1:653–661. [PubMed: 17802642]
50. Kohm AP, McMahon JS, Podojil JR, Begolka WS, DeGutes M, Kasprovicz DJ, Ziegler SF, Miller SD. Cutting Edge: Anti-CD25 monoclonal antibody injection results in the functional inactivation, not depletion, of CD4+CD25+ T regulatory cells. *J Immunol.* 2006; 176:3301–3305. [PubMed: 16517695]
51. Macauley MS, Pfrengle F, Rademacher C, Nycholat CM, Gale AJ, von Drygalski A, Paulson JC. Antigenic liposomes displaying CD22 ligands induce antigen-specific B cell apoptosis. *J Clin Invest.* 2013; 123:3074–3083. [PubMed: 23722906]
52. Hadeiba H, Sato T, Habtezion A, Oderup C, Pan J, Butcher EC. CCR9 expression defines tolerogenic plasmacytoid dendritic cells able to suppress acute graft-versus-host disease. *Nat Immunol.* 2008; 9:1253–1260. [PubMed: 18836452]
53. Zou W, Machelon V, Coulomb-L'Hermin A, Borvak J, Nome F, Isaeva T, Wei S, Krzysiek R, Durand-Gasselini I, Gordon A, Pustilnik T, Curiel DT, Galanaud P, Capron F, Emilie D, Curiel TJ. Stromal-derived factor-1 in human tumors recruits and alters the function of plasmacytoid precursor dendritic cells. *Nat Med.* 2001; 7:1339–1346. [PubMed: 11726975]
54. de Heer HJ, Hammad H, Soullie T, Hijdra D, Vos N, Willart MA, Hoogsteden HC, Lambrecht BN. Essential role of lung plasmacytoid dendritic cells in preventing asthmatic reactions to harmless inhaled antigen. *J Exp Med.* 2004; 200:89–98. [PubMed: 15238608]
55. Jongbloed SL, Benson RA, Nickdel MB, Garside P, McInnes IB, Brewer JM. Plasmacytoid dendritic cells regulate breach of self-tolerance in autoimmune arthritis. *J Immunol.* 2009; 182:963–968. [PubMed: 19124739]
56. Chen W, Liang X, Peterson AJ, Munn DH, Blazar BR. The indoleamine 2,3-dioxygenase pathway is essential for human plasmacytoid dendritic cell-induced adaptive T regulatory cell generation. *J Immunol.* 2008; 181:5396–5404. [PubMed: 18832696]
57. Jahrsdorfer B, Vollmer A, Blackwell SE, Maier J, Sontheimer K, Beyer T, Mandel B, Lunov O, Tron K, Nienhaus GU, Simmet T, Debatin KM, Weiner GJ, Fabricius D. Granzyme B produced by human plasmacytoid dendritic cells suppresses T-cell expansion. *Blood.* 2010; 115:1156–1165. [PubMed: 19965634]
58. Tel J, Sittig SP, Blom RA, Cruz LJ, Schreibelt G, Figdor CG, de Vries IJ. Targeting Uptake Receptors on Human Plasmacytoid Dendritic Cells Triggers Antigen Cross-Presentation and Robust Type I IFN Secretion. *J Immunol.* 2013
59. Tel J, Benitez-Ribas D, Hoosemans S, Cambi A, Adema GJ, Figdor CG, Tacke PJ, de Vries IJ. DEC-205 mediates antigen uptake and presentation by both resting and activated human plasmacytoid dendritic cells. *Eur J Immunol.* 2011; 41:1014–1023. [PubMed: 21413003]
60. Meyer-Wentrup F, Benitez-Ribas D, Tacke PJ, Punt CJ, Figdor CG, de Vries IJ, Adema GJ. Targeting DCIR on human plasmacytoid dendritic cells results in antigen presentation and inhibits IFN- α production. *Blood.* 2008; 111:4245–4253. [PubMed: 18258799]
61. St Pierre CA, Leonard D, Corvera S, Kurt-Jones EA, Finberg RW. Antibodies to cell surface proteins redirect intracellular trafficking pathways. *Exp Mol Pathol.* 2011; 91:723–732. [PubMed: 21819978]
62. Gavin MA, Clarke SR, Negrou E, Gallegos A, Rudensky A. Homeostasis and anergy of CD4(+)CD25(+) suppressor T cells in vivo. *Nat Immunol.* 2001; 3:33–41. [PubMed: 11740498]

63. Tai X, Van Laethem F, Pobeziński L, Guinter T, Sharrow SO, Adams A, Granger L, Kruhlak M, Lindsten T, Thompson CB, Feigenbaum L, Singer A. Basis of CTLA-4 function in regulatory and conventional CD4(+) T cells. *Blood*. 2012; 119:5155–5163. [PubMed: 22403258]
64. Lee KM, Chuang E, Griffin M, Khattri R, Hong DK, Zhang W, Straus D, Samelson LE, Thompson CB, Bluestone JA. Molecular basis of T cell inactivation by CTLA-4. *Science*. 1998; 282:2263–2266. [PubMed: 9856951]
65. Schneider H, Downey J, Smith A, Zinselmeyer BH, Rush C, Brewer JM, Wei B, Hogg N, Garside P, Rudd CE. Reversal of the TCR stop signal by CTLA-4. *Science*. 2006; 313:1972–1975. [PubMed: 16931720]
66. Rigby M, DiMeglio L, Rendell M, Felner E, Dostou J, Gitelman S, Patel C, Tsalikian G, Gottlieb P, Greenbaum C, Sherry N, Moore W, Monzavi R, Willi S, Raskin P, Moran A, Russell W, Pinckney A, Keyes-Elstein L, Howell M, Aggarwal S, Lim N, Phippard D, Nepom G, McNamara J, Ehlers M. Targeting of memory T cells with alefacept in new-onset type 1 diabetes (T1DAL study): 12 month results of a randomised, double-blind, placebo-controlled phase 2 trial. *Lanc Diab & Endo*. 2013; 1:284–294.

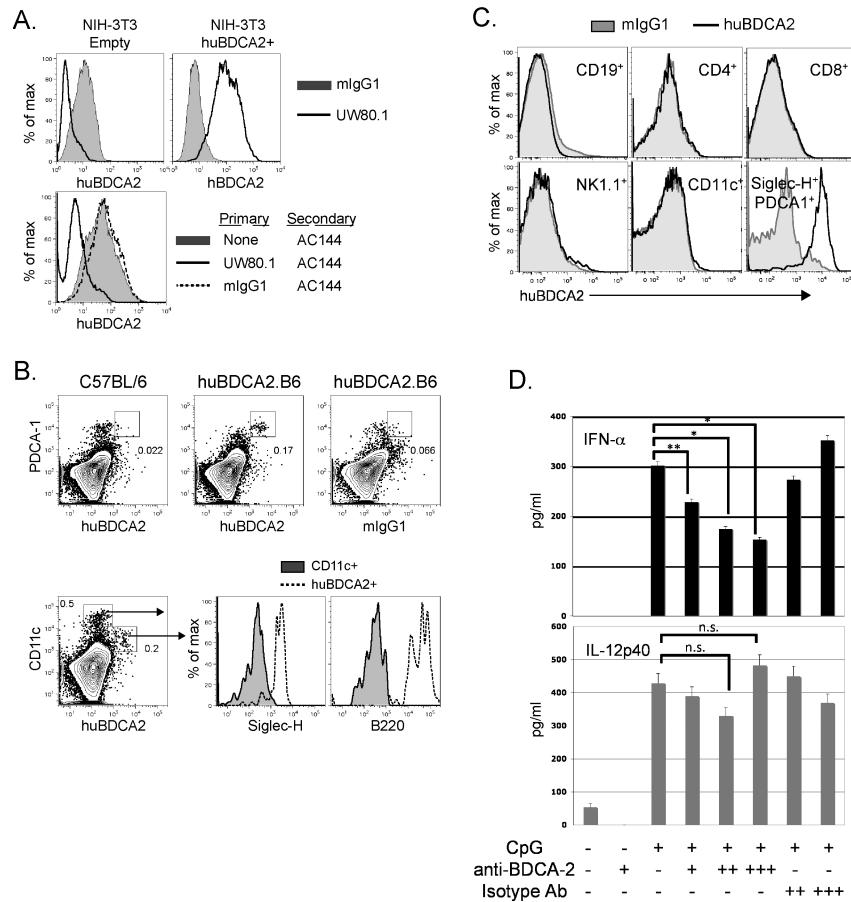


Figure 1. Characterization of anti-human BDCA2 mAbs and human BDCA2 transgenic mice
A, upper panel, NIH-3T3 cells transfected with BDCA2 or an empty vector control were stained with 10 μ g/ml anti-BDCA2 mAb, UW80.1 or mouse IgG1 isotype control (G28-1). *Lower panel*, NIH-3T3-BDCA2 transfectants were incubated with either UW80.1 anti-BDCA2, mIgG1 isotype control or left untreated. Following washes to remove unbound mAbs, cells were stained with 5 μ l PE-conjugated anti-BDCA2, (AC144). *B*, Analysis of pDC-specific expression of BDCA2. Splenocytes from control B6 or B6.BDCA2 transgenic mice were stained with fluorochrome-conjugated mAbs against CD11c, PDCA-1, Siglec-H, B220, and BDCA2 (UW80.1) or mIgG1 isotype control. *Upper panel* shows BDCA2 expression on PDCA-1⁺ pDCs from B6 and B6.BDCA2 Tg mice. *Lower panel* displays Siglec-H and B220 expression on BDCA2- and CD11c-gated cells from B6.BDCA2 Tg mice. Numbers in plots denote frequency among total scatter-gated splenocytes. Data shown are representative of >10 animals analyzed. *C*, Splenocytes from B6.BDCA2 Tg mice were stained with mAbs against CD19, CD4, CD8, NK1.1, CD11c, Siglec-H, PDCA-1, and BDCA2 or mIgG1 isotype control. Data shown are representative of 3 animals analyzed. *D*, Magnetically enriched pDCs from B6.BDCA2 Tg mice were stimulated in vitro with 10 μ g/ml CpG-A with or without 2 or 10 μ g/ml BDCA2 mAb (AC144) or mIgG1 isotype control (G28-1). 18 h later supernatants were collected and assayed for IFN- α and IL-12p40 by ELISA. Experiment shown is representative of 4 independent experiments.

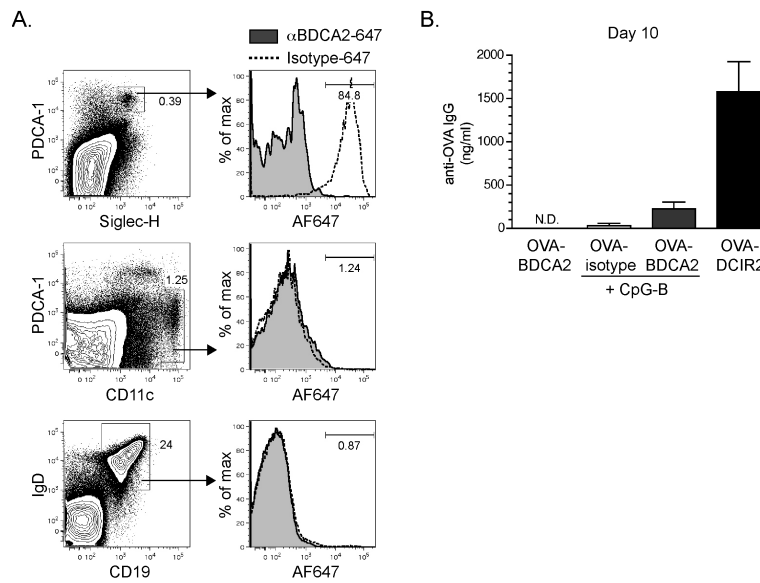


Figure 2. BDCA2 can serve as a target for Ag delivery in B6.BDCA2 mice

A. Groups of B6.BDCA2 mice were injected i.v. with 2 μ g AlexaFluor647-conjugated anti-BDCA2 (UW80.1) or mIgG1 isotype control and sacrificed one hour following injection. Splenocytes from injected mice were stained with mAbs specific for PDCA-1, Siglec-H, and CD11c, or IgD and CD19. Flow plots (*left*) depict gating for Siglec-H⁺PDCA-1⁺ pDCs (*upper*), CD11c⁺ myeloid DCs (*middle*), and CD19⁺IgD⁺ B cells (*bottom*). Numbers within flow plots denote frequency among total splenocytes. Histograms (*right*) show AlexaFluor647 fluorescence among the gated populations from anti-BDCA2-647-injected or mIgG1-647-injected mice. Numbers within histograms denote frequency of AlexaFluor647-positive cells among the gated population from mice that received anti-BDCA2-647. A representative experiment of five is shown using 2-3 mice/group.

B. Groups of B6.BDCA2 mice were immunized i.v. with 10 μ g OVA-conjugated anti-BDCA2, mIgG1 isotype control or anti-DCIR2 with or without 50 μ g CpG-A. Graph depicts mean \pm SEM of anti-OVA IgG in the serum 10 d post-immunization. A representative experiment of three is shown using 3-4 mice/group.

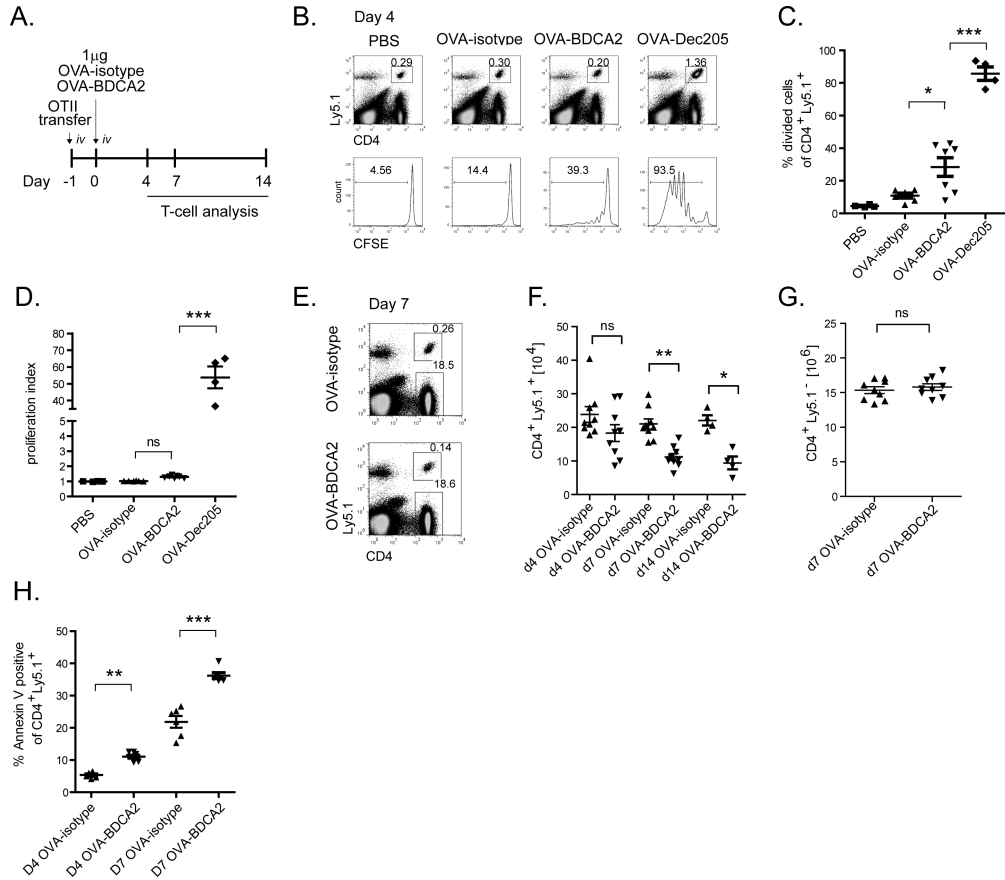


Figure 3. Targeting Ag to BDCA2⁺ pDCs leads to a reduction of Ag-specific T cells
A, Schematic for immunization and subsequent analysis. **B,** B6.BDCA2 recipients of CFSE-labeled OT-II cells were injected *i.v.* with PBS or 1 μg OVA-isotype, OVA-BDCA2 or OVA-DEC205 and sacrificed on d 4 following injection. Flow plots (top) depict gating of CD4⁺Ly5.1⁺ cells. Histograms (bottom) depict CFSE fluorescence among gated CD4⁺Ly5.1⁺ population in each group. **C-D,** Cumulative data from **B** showing the percentage of divided cells (**C**) and cell proliferation index (**D**) defined as total CFSE fluorescence (MFI) of PBS group divided by total CFSE fluorescence (MFI) for each group. Data in **B-D** are from 2 independent experiments using 2-4 mice per group. **E,** Cohorts of B6.BDCA2 recipients were immunized as in (**A**) and the frequency of CD4⁺Ly5.1⁺ and CD4⁺Ly5.1⁻ cells were determined at d 4. Numbers within flow plots denote frequency among total splenocytes. **F,** Scatter plots depict the total number of CD4⁺Ly5.1⁺ splenocytes from mice immunized as in (**A**) 4, 7 and 14 d post-immunization. Data in **E-F** are from three independent experiments using 3 mice/group. **G,** The number of endogenous CD4⁺ T cells per spleen 7 d p.i. from mice immunized as in (**A**) are plotted. **H,** The percentage of apoptotic cells within gated CD4⁺Ly5.1⁺ splenocytes at d 4 and d 7 was determined by AnnexinV staining in B6.BDCA2 recipients immunized as in (**A**). Data in **C, F** and **G** are pooled data from three independent experiments where each dot represents an individual animal with the mean indicated for each group (horizontal bars) ± SEM. Cell numbers in **F** and **G** were calculated based on the total cell number per spleen. * p<0.05, ** p<0.01, ***

$p < 0.001$, as determined by two-tailed, unpaired Student's t-test or one-way ANOVA with Tukey post-test.

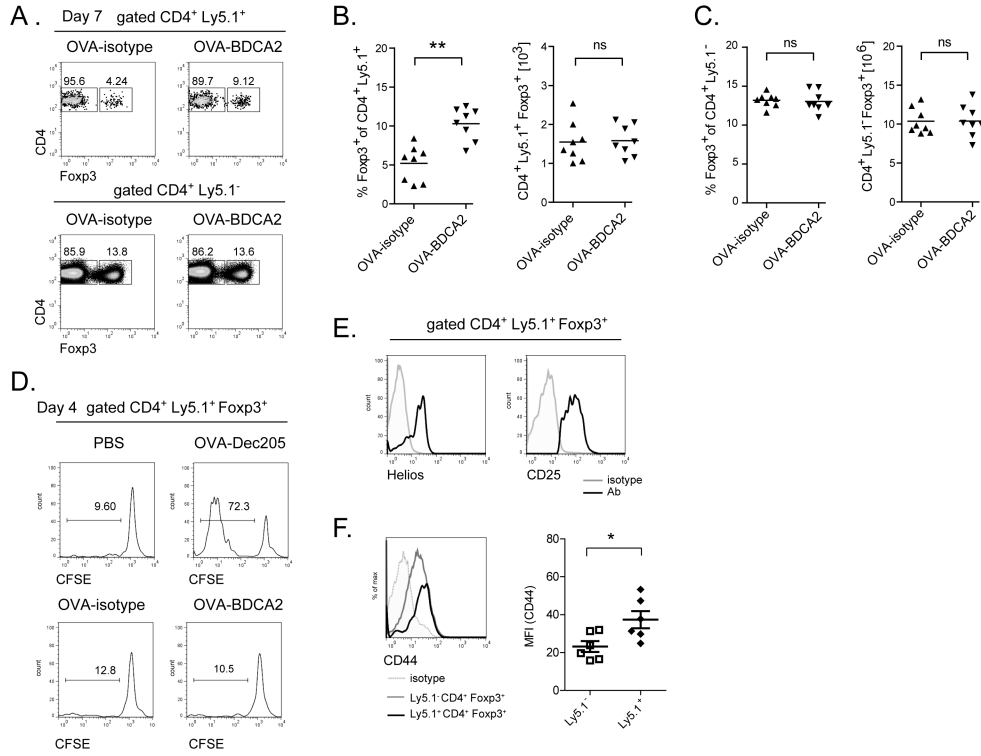


Figure 4. Targeting Ag to BDCA2⁺ pDCs leads to increased frequencies of Ag-specific T_{reg} cells A-C, Cohorts of B6.BDCA2 recipients were immunized as in (Fig. 3A) and sacrificed 7 d post-immunization. A, The frequency of Foxp3⁺ cells within CD4⁺Ly5.1⁺ and CD4⁺Ly5.1⁻ splenocytes is shown. B and C, Combined data from three independent experiments showing the frequency and number of Foxp3⁺CD4⁺Ly5.1⁺ (B) and Foxp3⁺CD4⁺Ly5.1⁻ splenocytes (C). D, Histograms depict CFSE dilution among gated Foxp3⁺CD4⁺Ly5.1⁺ splenocytes 4 d following immunization as indicated. E, Representative histograms show the expression of Helios and CD25 among gated Foxp3⁺CD4⁺Ly5.1⁺ cells 7 d p.i.. F, Representative histograms show CD44 expression among gated Foxp3⁺CD4⁺Ly5.1⁺ cells 7 d p.i. For B, C and F, each dot represents an individual animal with the mean indicated for each group (horizontal bars) ± SEM. Cell numbers in B and C were calculated based on the total cell number per spleen. * p<0.05, ** p<0.01, *** p<0.001, as determined by two-tailed, unpaired Student’s t-test or one-way ANOVA with Tukey post-test.

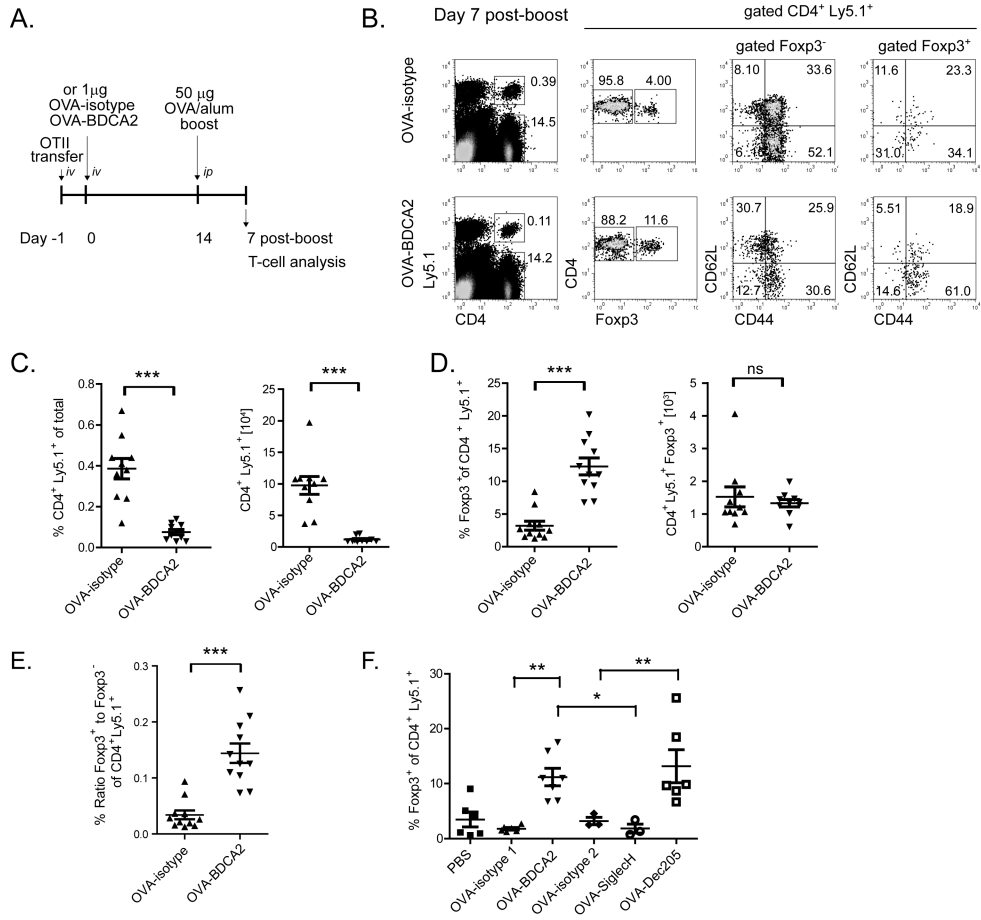


Figure 5. Ag delivery to BDCA2⁺ pDCs alters secondary T-cell responses and leads to increased frequencies of Foxp3⁺ T cells

A, Schematic for immunization and subsequent analysis for panels **B-E**. **B**, Flow plots depict gating strategy for analysis of CD44 and CD62L expression among transferred CD4⁺Ly5.1⁺ Foxp3⁻ and Foxp3⁺ splenocytes. Numbers in quadrants represent percentages within the gated population. **C**, Data showing the frequencies and numbers of CD4⁺Ly5.1⁺ cells. **D**, Scatter plots depict the frequency and number of Foxp3⁺ CD4⁺ Ly5.1⁺ cells. **E**, Scatter plots show the ratio of Foxp3⁺ CD4⁺ Ly5.1⁺ to Foxp3⁻ CD4⁺ Ly5.1⁺ splenocytes as defined in **B**. Data shown in **C**, **D** and **E** are pooled data from three independent experiments. Each dot represents an individual animal with the mean indicated for each group (horizontal bars) ± SEM. Cell numbers in **C** and **D** were calculated based on the total cell number per spleen. **F**. Cohorts of B6.BDCA2 recipients of OT-II T cells were injected with PBS, 1 µg OVA-isotype 1 (mouse IgG1), OVA-BDCA2, OVA-isotype 2 (rat IgG2a), OVA-SiglecH or OVA-DEC205; mice were otherwise treated as in **A** and analyzed as in **B**. Scatter plot depicts the frequency of Foxp3⁺CD4⁺Ly5.1⁺ splenocytes within each group. Data are pooled from two independent experiments. Each dot represents an individual animal with the mean indicated for each group (horizontal bars). * p<0.05, ** p<0.01, *** p<0.001, as determined by two-tailed, unpaired Student's t-test or one-way ANOVA with Tukey post-test.

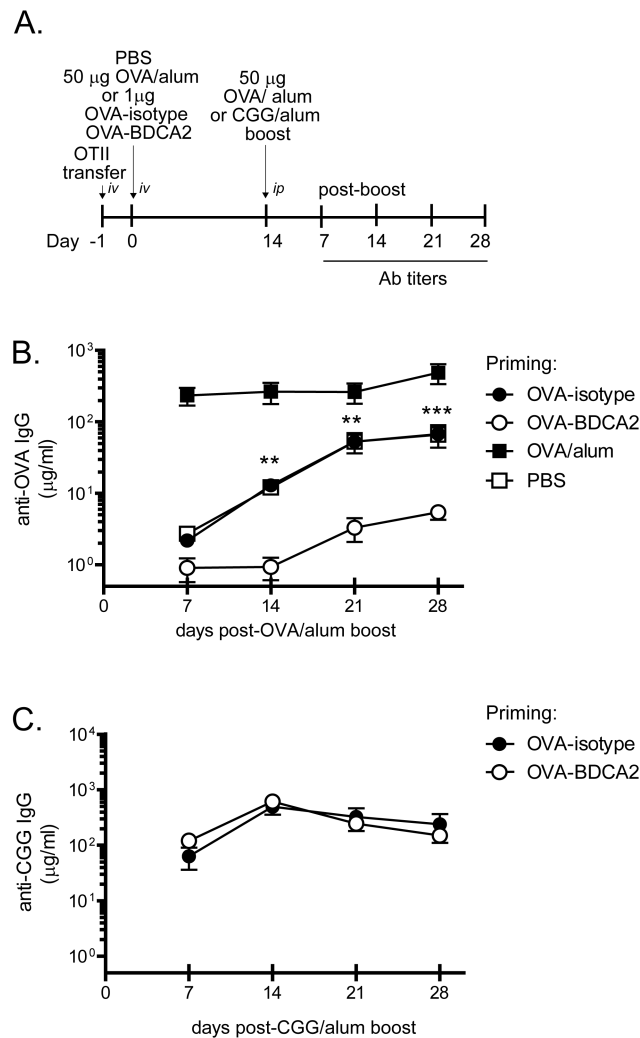


Figure 6. OVA-BDCA2 immunization suppresses Ag-specific Ab responses

A. Schematic for immunization and subsequent analysis. **B.** Cohorts of B6.BDCA2 recipients of OT-II T cells were primed with 1 µg OVA-BDCA2 or OVA-isotype, or given PBS or 50µg OVA plus alum one day following adoptive transfer. 14 d later mice were boosted with 50 µg OVA plus alum and then bled weekly for 4 wks to collect serum. Line graph depicts quantities of OVA-specific serum IgG as determined by ELISA. Data shown are a representative experiment of 3 independent experiments using 3-4 mice/group. **C.** B6.BDCA2 recipients of OT-II T cells were primed with 1 µg OVA-BDCA2 or OVA-isotype and challenged 14 d later with either 50 µg OVA or CGG plus alum and bled weekly for 4 wks to collect serum. Line graph shows quantities of OVA-specific serum IgG as determined by ELISA. A representative experiment of 3 independent experiments using 3-4 mice/group is shown.

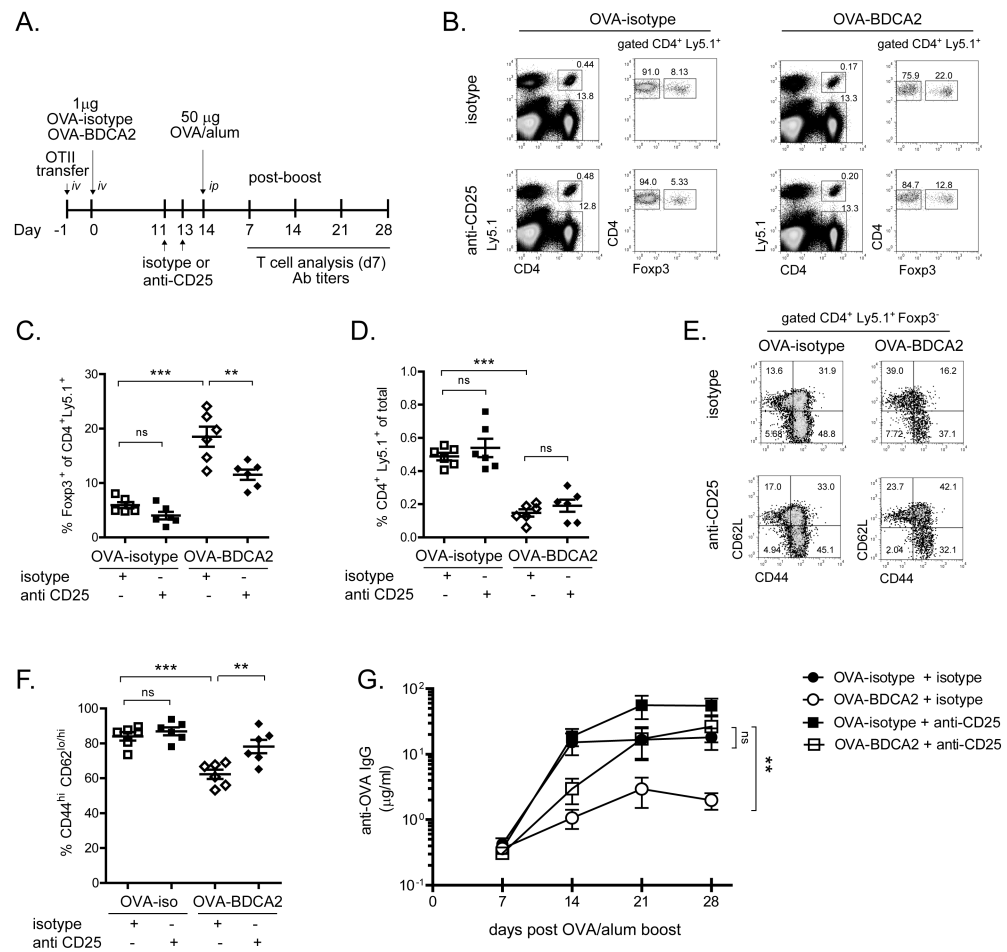


Figure 7. Depletion of T_{regs} by anti-CD25 Ab restores Ag-specific Ab responses following Ag re-challenge

A, Schematic for immunization, injections and subsequent analysis. B, Flow plots depict frequencies of CD4⁺Ly5.1⁺ and CD4⁺Ly5.1⁻ cells (among total splenocytes) and Foxp3⁺ and Foxp3⁻ cells (among gated CD4⁺Ly5.1⁺ cells) in mice given anti-CD25 or isotype control mAbs 8 d previously. C, Scatter plot showing the frequency of Foxp3⁺ cells among gated CD4⁺Ly5.1⁺ splenocytes for the indicated groups. D, Scatter plot showing the frequency of CD4⁺Ly5.1⁺ cells among total splenocytes for the indicated groups. E, Flow plots depicting CD44 and CD62L expression among gated Foxp3⁻ CD4⁺ Ly5.1⁺ splenocytes. F, Scatter plot depicts the combined frequency of activated CD44^{hi}CD62L^{hi/lo} cells gated in (E). Data in B-F are from three independent experiments using 2-3 mice/group. For C, D and F, each dot represents an individual animal with the mean indicated for each group (horizontal bars) \pm SEM. G, Line graph depicts quantities of OVA-specific serum IgG as determined by ELISA for the indicated groups. Data shown are the combined results from 3 independent experiments using 3-5 mice/group. * p<0.05, ** p<0.01, *** p<0.001, as determined by one-way ANOVA with Tukey post-test (B-F) or one-way ANOVA with repeated measures (G).

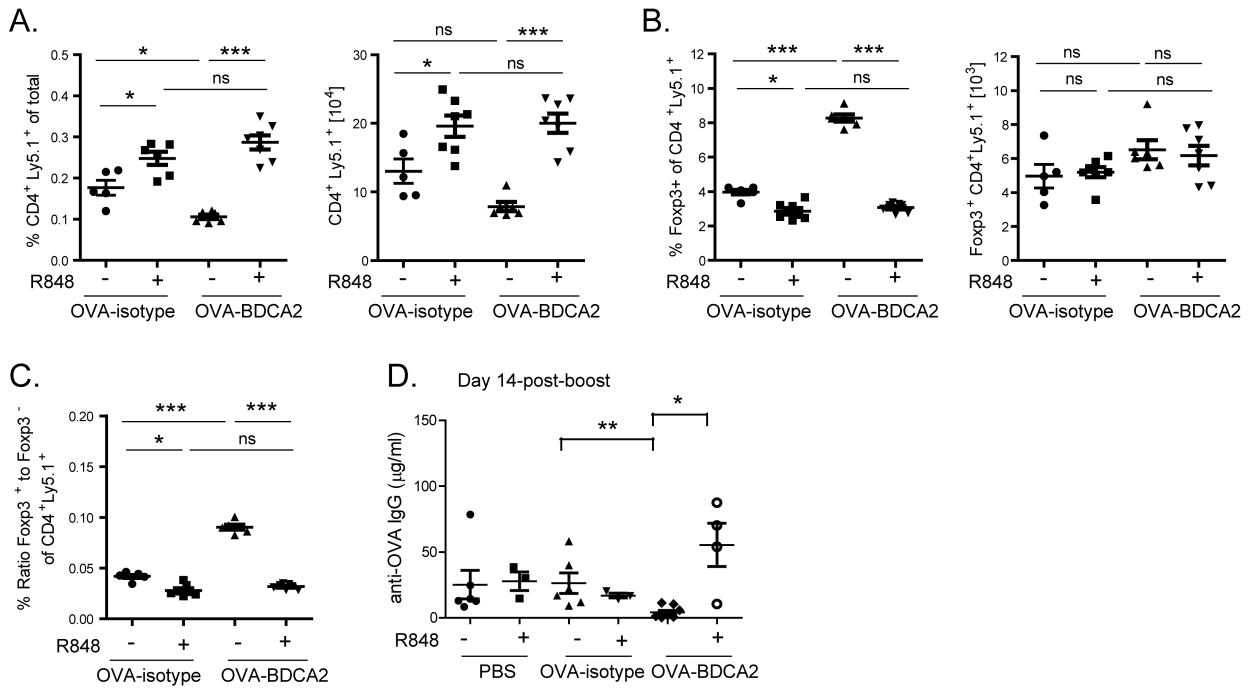


Figure 8. TLR7 agonist treatment at the time of Ag delivery prevents T_{eff} cell deletion and restores Ag-specific Ab responses following Ag re-challenge

Cohorts of B6.BDCA2 mice were immunized as in Fig. 3A with or without 50 μg R848. *A*, Scatter plots showing the frequency (left) and number (right) of total transferred Ly5.1⁺ CD4⁺ splenocytes for the indicated groups 7 d p.i. *B*, Scatter plots showing the frequency (left) and number (right) of Foxp3⁺ cells among CD4⁺ Ly5.1⁺ splenocytes quantified in *A*. *C*, Scatter plot depicts the ratio of the frequencies of Foxp3⁺ CD4⁺ Ly5.1⁺ to Foxp3⁻ CD4⁺ Ly5.1⁺ for the indicated groups at d 7 p.i. Data shown in *A-C* are from 2 independent experiments using 3-4 mice/group. Each dot represents an individual animal with the mean indicated for each group (horizontal bars) ± SEM. Cell numbers were calculated based on the total cell number per spleen. *E*. Line graph shows the quantity of OVA-specific serum IgG for the indicated groups as determined by ELISA. One representative experiment of three independent experiments using 3-5 mice/group is shown. Each dot represents an individual animal with the mean indicated for each group (horizontal bars) ± SEM. * p<0.05, ** p<0.01, *** p<0.001, as determined by one-way ANOVA with Tukey post-test.